Burn-in free non-fullerene based organic solar cells

Nicola Gasparini[1*], Michael Salvador[1,2], Sebastian Strohm[1,3], Thomas Heumueller[1], Ievgen Levchuk[1], Andrew Wadsworth[4], James H. Bannock[4], John C. de Mello[4], Hans-Joachim Egelhaaf[3], Derya Baran[5], Iain McCulloch[4,5] and Christoph J. Brabec[1,3*]

[1]Institute of Materials for Electronics and Energy Technology (I-MEET), Friedrich-Alexander-University Erlangen-Nuremberg, Martensstraße 7, 91058 Erlangen, Germany

[2]Instituto de Telecomunicações, Instituto Superior Técnico, Av. Rovisco Pais, P-1049-001 Lisboa, Portugal

[3]Bavarian Center for Applied Energy Research (ZAE Bayern), Haberstrasse 2a, 91058 Erlangen, Germany

[4]Department of Chemistry and Centre for Plastic Electronics, Imperial College London, London,SW7 2AZ, UK

[5]King Abdullah University of Science and Technology (KAUST), KAUST Solar Center (KSC), Thuwal 23955-6900, Saudi Arabia

N.G. and M.S. contributed equally to this work

Organic solar cells; non-fullerene acceptor; light-soaking stability; degradation; P3HT

ABSTRACT

Organic solar cells that are free of *burn-in*, the commonly observed rapid performance loss under light, are presented. The solar cells are based on poly(3-hexylthiophene) (P3HT) with varying molecular weights and a non-fullerene acceptor (IDTBR) and were fabricated in air. P3HT:IDTBR solar cells light-soaked over the course of 2000 h lose about 5% of power conversion efficiency (PCE), in stark contrast to PCBM-based solar cells whose *PCE* shows a burn-in that extends over several hundreds of hours and levels off at a loss of ~34%. Replacing PCBM with IDTBR prevents short-circuit current losses due to fullerene dimerization and inhibits disorder induced open circuit voltage losses, indicating a very robust device operation that is insensitive to defect states. Small losses in fill factor over time are proposed to originate from polymer or interface defects. Finally, the combination of enhanced efficiency and stability in P3HT:IDTBR increases the lifetime energy yield by more than a factor of ten when compared with the same type of devices using a fullerene-based acceptor instead.

With many groups now consistently reporting single junction organic solar cells with power conversion efficiencies well above the psychologically important 10% threshold this technology is becoming increasingly competitive with other thin-film photovoltaic technologies.[1,2] On the down side, the device longevity remains a critical problem and attention needs to be directed towards understanding and solving the current lifetime limitations. It is well established that environmental factors such as oxygen and water in the presence of light can lead to irreversible performance breakdown mostly due to photooxidation of the active layer and corrosion of the metal electrode.[3,4] However, even in the absence of these extrinsic factors, i.e., in the case of firmly packaged devices, short and long-term photovoltaic performance loss is still observed under operation.[5,6] A particularly severe phenomenon is the so-called light-induced or temperature induced *burn-in* – a term that originates from common practice in semiconductor devices referring to the application of electrical or temperature stress in order to detect or mitigate early failures.[7] In organic polymer based solar cells, the burn-in period reflects an early, near to exponential photovoltaic performance roll-off.[8] The effect may deplete the initial power conversion efficiency by as much as 20 – 60%,[9] depending on the material system. It typically occurs so rapidly that it is generally accepted to specify the lifetime of the device post burn-in phase, i.e., neglecting the early loss in performance.[10] This intrinsic, light-driven degradation observation is thought to be mostly determined by material properties of the active layer and less due to interfaces and electrodes.[9,10] For instance, light-induced burn-in has been experimentally and theoretically correlated, although to different extent, with photochemical reactions,[11] critical concentrations of chemical and metal impurities,[12,13] molecular weight distribution,[14] degree of crystallinity,[15] crosslinking,[16] processing additives,[17] and the formation of long-lived radicals.[18] In light of these considerations, current state of the art envisions photovoltaic materials with elevated levels of photostability and high degree of purity and crystallinity, ideally free of radical-forming processing additives. It thus appears

forthcoming to consider conjugated polymers of low structural complexity and relatively inert functional building blocks that tend to adopt a very ordered microstructure in thin films. The prototypical homo-polymer P3HT combines those characteristics. Yet, when blended with common C60 fullerene acceptors, P3HT, in addition to the rather low power conversion efficiency, may feature a significant burn-in loss, primarily in short-circuit current, which has been linked to the formation of fullerene dimers.[19,20] While fullerene oligomerization can be alleviated using, e.g., C70 based fullerenes or higher fullerene adducts, solution-processed organic solar cells without burn-in remain unprecedented. As such, replacing the fullerene acceptor by non-fullerene molecules constitutes one prospective route towards organic solar cells with enhanced long-term operational stability. Recently, we presented non-fullerene acceptor molecules based on rhodanine-benzothiadiazole-coupled indacenodithiophene (IDTBR) that yield efficiencies close to 8% when blended with P3HT in ternary devices.[21,22] Blends of P3HT:IDTBR feature high degree of crystallinity,[21] commensurate with the stability criteria established above, leading to improved shelf-life and photo-oxidation stability.[21,22] Given the ease with which P3HT can be scaled up this result represents an important avenue for large area, low-cost deployment of organic photovoltaics. In this work, we studied the intrinsic stability of P3HT:IDTBR (the latter in the form of its n-octyl side chain variation also known as O-IDTBR[21], **Figure 1b**) solar cells when exposed in an inert environment to white light irradiation, mimicking firmly packaged devices. Significantly, we found that P3HT:IDTBR bulk heterojunction solar cells are predominantly free of photo-induced burn-in. As opposed to P3HT:PCBM solar cells run in parallel, this novel blend shows no losses in short-circuit current and open circuit voltage and a minor drop in fill factor. We elucidate the photophysics and microscopic structure of P3HT:IDTBR bulkheterojunction (BHJ) solar cells and conclude that this blend shows superior resistance towards prolonged light soaking. We emphasize the relevance and generality of this result by showing similar burn-in free behavior in devices consisting of active layers with different batches of P3HT

featuring different molecular weights. Our results inform that non-fullerene acceptors could be key in achieving high efficiency organic solar cells with long-term stable device performance.

For studying the intrinsic stability and specifically the photo-induced burn-in in P3HT:IDTBR based devices, we fabricated organic BHJ solar cells in an inverted device configuration consisting of ITO/ZnO/active layer/PEDOT:PSS/Ag, with all layers except the top metal contact doctor bladed in air. **Figure 1a** and **Figure 1b** show the device layout and the chemical structure of the photoactive materials, respectively, used in this work. In agreement with our previous reports[23], P3HT:IDTBR devices delivered a power conversion efficiency (PCE) of 6.05% under simulated solar illumination based on 0.72 V of open circuit voltage (V_{oc}), 12.55 mAcm^{-2} of short circuit current density (J_{sc}) and a fill factor (FF) of 0.67. We fabricated in parallel reference solar cells made of P3HT:PCBM with state-of-the-art photovoltaic parameters (**Table 1**)[24].

Upon device fabrication, the solar cells were placed in a sealed, electronically controlled degradation chamber with regulated environment (O_2 < 1ppm, H_2O < 1ppm, **Figure S1** in Supporting Information). The *J-V* characteristics of both PCBM and IDTBR based devices were probed periodically while continuously light-soaked using white light LEDs (**Figure S2**) irradiating at 100 mW/cm^2. The motivation for this type of LEDs is to avoid heating effects as well as simulate the use of a UV filter, a critical factor for attaining long-term stability given the propensity for UV-induced radical reactions in conjugated polymers.[11,25] **Figure 1c** depicts the current-voltage behavior under solar simulator light for both types of solar cells before and after 2000 h of accelerated lifetime testing under open circuit, while **Figure 2** shows the temporal evolution of all photovoltaic parameters. Notably, in the case of aged non-fullerene based devices the FF is the only photovoltaic parameter that experiences a significant drop of ~10%, while V_{oc} remains unaffected and J_{sc} slightly increases (~4%) when compared with time zero. Overall, light-soaked P3HT:IDTBR solar

cells lose about 5% of power conversion efficiency in the course of 2000 h of light exposure. Importantly, the power output of P3HT:IDTBR based devices is burn-in free, i.e., it does not show the typical exponential performance loss. Instead, *PCE* decreases gradually as a function of the time of exposure. The elevated intrinsic photo-stability of P3HT:IDTBR solar cells reflects one of the most stable long-term behaviors observed to date for solution-processed solar cells under accelerated lifetime testing.[9,10,26] This is in stark contrast to PCBM-based solar cells whose *PCE* shows a burn-in that extends over several hundreds of hours and levels off at a loss of ~34% (2% V_{oc}, 27% J_{sc} and 7% FF loss). We confirmed the current density values obtained from *J-V* traces by performing external quantum efficiency (EQE) measurements. **Figure 1d** depicts the EQE profiles of P3HT:IDTBR and P3HT:PCBM before and after light soaking. We note that the integrated EQE for these devices matches the measured J_{sc} with a margin of less than 5%, confirming the severe current losses in aged P3HT:PCBM devices and improved J_{sc} in aged P3HT:IDTBR solar cells. Interestingly, the increase in EQE originates from spectral regions that can be linked to IDTBR rather than P3HT.

As a means to quantify the stability benefit achieved by replacing PCBM with IDTBR we adopted the performance metric by *Roesch et al*. to calculate the lifetime energy yield (LEY).[10] The LEY represents the output power of a solar cell for a given temporal decay curve of *PCE* assuming constant 1 sun irradiation. Analyzing the traces in **Figure 2d** and defining T_{80} (time at which the performance drops to 80% of the initial value) as the lifetime yields 230 kWh m^{-2} and 9.2 kWh m^{-2} for IDTBR and PCBM-based devices, respectively. Given that in the case of P3HT:PCBM T_{80} falls into the burn-in period, it is common to define T_{S80}, i.e., a stabilized T_{80} lifetime after the burn-in (see **Figure S3** and supplementary information for details; note that T_{S80} does not exist for P3HT:IDTBR). In this case, LEY extends to 61.4 kWh m^{-2}. Even under this – for P3HT:PCBM – more favorable analysis, the combination of superior lifetime and efficiency translates into a maximum energy yield that is

a factor of three larger in the case of P3HT:IDTBR. We emphasize that the lifetime traces for P3HT:IDTBR shown in **Figure 2** represent average values obtained from three different batches of P3HT featuring very different molecular weights. The photovoltaic traces resolved by molecular weight are shown in **Figure S4**. Importantly, none of these different polymer batches shows an apparent burn-in; neither do we observe a clear stability trend as a function of the molecular weight.[14,27] In all cases, the PCE decreases gradually and drops between 2 and 10% after 2000 h. In analogy to the results shown in **Figure 2**, the drop in PCE is solely determined by a loss in FF (**Figure S4a**). These results anticipate that non-fullerene acceptors could provide inherent photostability and grant general long-term device performance to solution-processed organic solar cells.

We now focus on the loss mechanisms of both types of solar cells. The intrinsic degradation paths of polymer-PCBM-based and P3HT:PCBM solar cells in particular are rather well understood.[28–31] In similar cases, the strongly reduced short circuit current has been quantitatively reproduced by mixing isolated fullerene dimers into a fresh mixture of a polymer-fullerene blend.[19] Fullerene dimers are thought to inhibit exciton splitting at the polymer-fullerene interface as well as induce exciton trapping in the fullerene phase.[32] Voltage losses while not clearly assigned to chemical degradation motifs are associated with an increase in energetic disorder on the polymer due to defect states.[28,33,34] Those states are likely to increase the charge carrier recombination rate and thus decrease the FF. Conversely, a clear picture of the photophysical mechanisms occurring in photoaged non-fullerene based solar cells is missing. Significantly, the different degradation kinetics of P3HT:PCBM and P3HT:IDTBR devices apparent from **Figure 2** anticipate different degradation processes.

We carried out additional current-voltage and transient photovoltage measurements to elucidate photovoltaic loss mechanisms due to photo-induced aging. We first considered the recombination dynamics by probing the current-voltage behavior at different light intensities for fresh and degraded solar cells (**Figure 3a-c** and **S5**). This technique is particularly useful

because J_{sc} generally follows a power law dependence on light intensity according to $J_{sc} \propto P_{in}^{S}$, where S represents a power law exponent and P_{in} the light intensity.[35–37] A linear dependence, i.e. S=1, is indicative of 2nd order recombination having a negligible effect on the extracted current, whereas S<1 suggests 2nd order recombination as a limiting factor. Conversely, in the case of V_{oc}, it has been shown that light-induced V_{oc} losses can be associated with trap state formation. Following theoretical considerations, trap-assisted recombination is identified by a slope of 2kT/q (at 300 K) in a semi-logarithmic plot of V_{oc} vs. light intensity, while a slope in the order of kT/q is a signature of purely 2nd order recombination.[38,39] From the comparative, double logarithmic J_{sc} vs light intensity representations in **Figures 3a** and **3b** it is apparent that the slope is unity and is not influenced by light exposure in the IDTBR-based system, i.e., charge carrier recombination at short-circuit is not limited by 2nd order recombination. P3HT:PCBM solar cells, on the other hand, feature S=0.91 and S=0.83 for fresh and aged devices, respectively, suggesting that in this semiconducting blend the extracted current becomes more and more limited by 2nd order recombination upon light soaking . Considering now the V_{oc} vs. light intensity plot in **Figure 3c**, the pristine solar cells feature a slope of 1.1 kT/q, i.e., almost pure 2nd order recombination, whereas we find slopes of 1.4 and 1.5 kT/q for aged IDTBR and PCBM-based devices, respectively, indicative of trap-assisted recombination of less than 2nd order. Thus, photoinduced degradation affects the recombination behavior in both types of devices due to trap state formation.

To further examine the impact of light exposure on charge generation and charge transport, we measured the photocurrent density (J_{ph}) as a function of the effective voltage (V_{eff}) as well as the charge carrier mobility. The J_{ph} vs. V_{eff} traces in **Figure 3d** indicate that J_{ph} quickly saturates for V_{eff} below ~1 V. Under this condition all photogenerated electron-hole pairs are likely to be dissociated and collected at the electrodes. This allows to estimate the maximum generation rate of free charge carriers G_{max} according to $J_{sat}=qG_{max}L$, where q is

the electronic charge and L is the active layer thickness.[40] G_{max} is slightly enhanced upon photoaging from $4.08x10^{21}$ $cm^{-3}s^{-1}$ to $4.43x10^{21}$ $cm^{-3}s^{-1}$ for P3HT:IDTBR devices. The enhancement of G_{max} is consistent with the improved J_{sc} values extracted under solar simulator illumination after photodegradation. The same analysis yields G_{max} values of $3.05x10^{21}$ $cm^{-3}s^{-1}$ and 2.43 $x10^{21}$ $cm^{-3}s^{-1}$ for fresh and aged P3HT:PCBM solar cells, respectively, confirming that the losses in J_{sc} are, at least partially (~20%), determined by reduced charge carrier generation. The shape of J_{ph} vs. V_{eff} allows additional conclusions with respect to the FF when considering the generation rate of free charge carriers at the voltage corresponding to the maximum power point of the *J-V* curve ($G_{MPP(V_{MPP})}$). It is apparent that $G_{MPP(V_{MPP})}$ is more strongly suppressed upon light aging for IDTBR-based devices, which matches the more pronounced loss in FF (**Table 1, Figure 2c**). This means that photodegradation has a significant influence on charge dissociation and extraction when operated under M_{PP} condition, which is of general practical relevance.

We now focus on understanding the impact of photo-induced aging on the charge transport behavior of P3HT:IDTBR and P3HT:PCBM-based devices. For this purpose, we investigated the charge carrier mobility (μ) of solar cells by employing the technique of photoinduced charge carrier extraction by linearly increasing voltage (photo-CELIV[41]) (see methods for further details). **Figure S6** displays the photo-CELIV traces of fresh and degraded devices. Notably, for PCBM and IDTBR blends, the maximum of the extraction peak (t_{max}) shifts towards larger extraction times for light soaked solar cells, corresponding to a decrease in carrier mobility by a factor of 1.9 and 1.8 for IDTBR and PCBM, respectively (**Table 1**). The values for μ and the broader extraction peaks in aged solar cells are indicative of trap state formation and longer carrier lifetimes, consistent with the V_{oc} – light intensity behaviour in **Figure 3c**.[42] This observation motivated a closer look into the recombination mechanism using transient photovoltage (TPV) and charge extraction techniques (CE) in

order to accurately calculate the charge carrier lifetime τ and charge carrier density n, respectively. In both measurements, the devices are operated under V_{oc} condition using different background illumination (from 0.2 to 2 suns) (see **Figure S7** and **Figure S8**).[43] Making use of the expression $\tau = \tau_0 \left(\frac{n_0}{n}\right)^{\lambda}$, where τ_0 and n_0 are constant factors, we can extract the recombination exponent (λ), which is a measure for the recombination order R (R=λ+1).[44] **Figure 4** displays τ *vs.* n for fresh and aged IDTBR and fullerene-based devices. We calculate a recombination order of 2.1 and 2.7 for pristine and photo-aged P3HT:IDTBR, respectively, and 2.3 and 3.0 in the case of P3HT:PCBM. As such, in both cases photo-aging induces a deviation from an ideal 2nd order recombination (R=2) behaviour. We attribute the enhanced recombination order to the aforementioned trap state formation in aged solar cells. In addition, the higher recombination order in the case of P3HT:PCBM devices provides an explanation for the slight drop in V_{oc} during light soaking (**Figure 1b**), underscoring more disordered charge transport in the bulk active layer.[42]

At this point, we understand that light-induced defects are causing a loss in FF in IDTBR-based devices. Still, the question of the origin and chemical nature of those traps remains. Fullerene oligomerization is intrinsically turned off as a potential loss mechanism in the case of the IDTBR blend. We also excluded a UV light soaking effect associated with ZnO as limiting factor by applying UV light at the end of the aging experiments – yielding no change in FF. To understand whether other structural changes in the bulk photoactive layer may explain the loss in FF we carried out UV-VIS, FTIR and XRD measurements on films of pristine and photoaged P3HT:IDTBR blends (**Figure S9-11**). Crucially, none of these techniques informs an elucidating change upon hundreds of hours of light exposure. We thus conclude that either the structural/chemical change associated with the observed traps is too small to be detected by these techniques or electronic traps are likely to be localized at the active layer interface. The latter is not unusual and has been observed in several material

systems.[45,46] At this point, it is worth noting that P3HT:IDTBR blends feature a distinct morphology, different from P3HT:PCBM.[21,22] While P3HT:PCBM is known to form a three-phase system, in which fullerene mixes into P3HT to decrease the crystallinity of the polymer phase,[47] we have shown in previous work that P3HT:IDTBR forms purer domains with sharper interfaces, preserving the crystallinity of P3HT. It is plausible that this peculiar morphology with higher polymer crystallinity in the case of P3HT:IDTBR is a chief aspect of its enhanced stability. In fact, earlier work has shown that crystalline polymers are less prone to light-induced traps and associated loss in photovoltaic perormance.[28]

In conclusion, we present fully-solution processed organic solar cells (only metal electrode is evaporated) based on the non-fullerene acceptor IDTBR that are free of the – for polymer-fullerene devices – typical early performance loss, the so-called photo-induced burn-in. We relate the absence of burn-in in the IDTBR blend to the fact that fullerene, which is prone to dimerization, could be replaced with an alternative acceptor. Disorder induced open circuit voltage losses, which are another common cause of burn-in, are also absent, indicating a very robust device operation that is insensitive to defect states. A small fill factor loss over time is observed in both, the devices with IDTBR and PCBM. We hypothesize that those may originate from polymer or interface defects. We anticipate that a better understanding of the active layer interface in polymer:non-fullerene devices as well as employing polymers with improved photofastness is likely to inhibit these loss channels, rendering these devices even more stable. The absence of burn-in removes the need for a *stabilized lifetime* and allows indexing the predicted lifetime to the time zero performance. Given that P3HT:IDTBR solar cells can achieve a power conversion efficiency beyond 6%, the combination of superior efficiency and stability allows to considerably boost the lifetime energy output. As an outlook, we envision that the future design of non-fullerene acceptors will bring about the missing key parameter in organic thin-film semiconductor blends that will combine improved photovoltaic performance with enhanced performance longevity. The presence of photoactive layers with

relatively pure, crystalline phases and sharp polymer/non-fullerene interphases could be one critical link.

Experimental Section

Materials. The P3HT batches of 68 kg mol^{-1} (PDI 1.6) and 94 kg mol^{-1} (PDI 1.6) weight-average molecular weight were synthesised by Grignard metathesis (GRIM) polymerisation in a droplet-flow reactor using a catalyst system developed for flow-based GRIM polymerisation.[48] A further P3HT batch of 134 kg mol^{-1} (PDI 1.6) molecular weight was synthesised using conventional flask methods.[49] Polymers were purified using a modification of the method reported by Bannock et al. [49], using a ternary mixture of acetone, ethyl acetate and hexane to remove impurities and oligomers from the polymer. IDTBR was synthetized as reported elsewhere. [21]

Device fabrication and measurements. Pre-structured indium tin oxide (ITO) substrates were cleaned with acetone and isopropyl alcohol in an ultrasonic bath for 10 minutes each. After drying, the substrates were doctor bladed with 40 nm of zinc oxide (ZnO) and a ~300 nm thick active layer based on P3HT:IDTBR (30 g L-1 in a mixture of Chlorobenzene (CB) and 4-Bromoanisole 95 to 5 vol %), followed by 15 nm of PEDOT:PSS (Al 4083). To complete the fabrication of the devices 100 nm of Ag were thermally evaporated through a mask (with a 10.4 mm^2 active area opening) under a vacuum of ~1x10-6 mbar. The J-V characteristics were measured using a source measurement unit from a homemade setup. Illumination was provided by a solar simulator (Oriel Sol 1A, from Newport) with AM1.5G spectrum at 100 mW cm-2. In order to study the light intensity dependence of current density, we used a series of neutral color density filters. The intensity of light transmitted through the filter was independently measured via a power meter. UV-VIS absorption was performed on a Lambda 950, from Perkin Elmer. EQEs were measured using an integrated system from Enlitech, Taiwan. All the devices were tested in ambient air.

Photo-CELIV measurements. The devices were illuminated using a 780 nm laser-diode. Current transients were recorded across an internal 50 Ω resistor of an oscilloscope (Agilent Technologies DSO-X 2024A). We used a fast electrical switch to isolate the cell and prevent charge extraction or sweep out during the laser pulse and the delay time. After a variable delay time, a linear extraction ramp is applied via a function generator. The ramp, which was 60 µs long and 2V in amplitude, was set to start with an offset matching the Voc of the cell for each delay time. From the measured photocurrent transients, the charge carrier mobility (µ) can be calculated using the following equation (1):

$$\mu = \frac{2d^2}{3At_{max}^2\left[1+0.36\frac{\Delta j}{j(0)}\right]} \; if \; \Delta j \leq j0, \qquad (1)$$

where d is the active layer thickness, A is the voltage rise speed A=dU/dt, U is the applied voltage, tmax is the time corresponding to the maximum of the extraction peak, and j(0) is the displacement current.

TPV and CE measurements. A 405 nm laser-diode was settled for keeping the solar cells at approximately V_{oc} condition. Driving the laser intensity with a waveform generator Agilent 33500B and measuring the light intensity with a highly linear photodiode allowed to reproducibly adjust the light intensity with an error below 0.5% over a range of 0.2 to 4 suns. A small perturbation was induced with a second 405 nm laser diode adjusted with a function generator from Agilent. The intensity of the short (50 ns) laser pulse was controlled to keep the voltage perturbation below 10 mV, typically at 5 mV. After the pulse, the voltage decays back to its steady state value in a single exponential decay. The characteristic decay time was determined from a linear fit to a logarithmic plot of the voltage transient and returned the small perturbation charge carrier lifetime. In charge extraction measurements a 405 nm laser diode illuminated the solar cell for 200 µs which was sufficient to reach a constant open-circuit voltage with steady state conditions. At the end of the illumination period, an analog

switch was triggered that switched the solar cell from open-circuit to short-circuit (50 Ω) conditions within less than 50 ns, allowing to quickly sweep out photogenerated carriers.

TPV, CE and photo-CELIV were measured using the Transient Measurement Unit from Automatic Research GmbH

FTIR. FTIR measurements were performed using a VERTEX-70 spectrometer (Bruker Optik GmbH). For this purpose, films of P3HT:IDTBR were coated on ZnSe substrates and degraded under the same conditions as full devices.

XRD. X-ray diffraction analysis was performed in classical ex situ Bragg–Brentano geometry using a Panalytical X'pert powder diffractometer with filtered Cu-Kα radiation and an 'Celerator solid-state stripe detector. Blend films of P3HT:IDTBR were bladed on glass substrates and degraded under the same conditions as full devices.

Acknowledgements

The authors gratefully acknowledge the support of the Cluster of Excellence ‘‘Engineering of Advanced Materials’’ at the University of Erlangen-Nuremberg, which is funded by the German Research Foundation (DFG) within the framework of its ‘‘Excellence Initiative’’, Synthetic Carbon Allotropes (SFB953) and Solar Technologies go Hybrid (SolTech). M. S. acknowledges primary support from a fellowship by the Portuguese Fundação para a Ciência e a Tecnologia (SFRH/BPD/71816/2010).The authors wish to thank Dr. Siva Krishnadasan (Department of Chemistry, Imperial College London) for assistance in the preparation of P3HT and Dr. Florian Machui (ZAE Bayern) for fruitful discussions for device preparation.

References

[1] H. Kang, G. Kim, J. Kim, S. Kwon, H. Kim, K. Lee, *Adv. Mater.* **2016**, *28*, 7821.

[2] M. A. Green, K. Emery, Y. Hishikawa, W. Warta, E. D. Dunlop, *Prog. Photovoltaics Res. Appl.* **2016**, *24*, 905.

[3] B. M. O. Reese, A. M. Nardes, B. L. Rupert, R. E. Larsen, D. C. Olson, M. T. Lloyd, S. E. Shaheen, D. S. Ginley, G. Rumbles, N. Kopidakis, **2010**, 3476.

[4] K. Norrman, M. V Madsen, S. A. Gevorgyan, F. C. Krebs, V. Frederiksborg, D.-Roskilde, *J. Am.Chem. Soc.* **2010**, *132*, 16883.

[5] C. H. Peters, I. T. Sachs-Quintana, J. P. Kastrop, S. Beaupré, M. Leclerc, M. D. McGehee, *Adv. Energy Mater.* **2011**, *1*, 491.

[6] J. Adams, G. D. Spyropoulos, M. Salvador, N. Li, S. Strohm, L. Lucera, S. Langner, F. Machui, H. Zhang, T. Ameri, M. M. Voigt, F. C. Krebs, C. J. Brabec, *Energy Environ. Sci.* **2015**, *8*, 169.

[7] J. A. Hauch, P. Schilinsky, S. A. Choulis, R. Childers, M. Biele, C. J. Brabec, *Sol. Energy Mater. Sol. Cells* **2008**, *92*, 727.

[8] C. H. Peters, I. T. Sachs-Quintana, W. R. Mateker, T. Heumueller, J. Rivnay, R. Noriega, Z. M. Beiley, E. T. Hoke, A. Salleo, M. D. McGehee, *Adv. Mater.* **2012**, *24*, 663.

[9] W. R. Mateker, M. D. McGehee, *Adv. Mater.* **2017**, *29*, 1603940.

[10] R. Roesch, T. Faber, E. Von Hauff, T. M. Brown, M. Lira-Cantu, H. Hoppe, *Adv. Energy Mater.* **2015**, *5*, 1.

[11] S. Shah, R. Biswas, *J. Phys. Chem. C* **2015**, *119*, 20265.

[12] C. Bracher, H. Yi, N. W. Scarratt, R. Masters, A. J. Pearson, C. Rodenburg, A. Iraqi, D. G. Lidzey, *Org. Electron.* **2015**, *27*, 266.

[13] J. Kuwabara, T. Yasuda, N. Takase, T. Kanbara, *ACS Appl. Mater. Interfaces* **2016**, *8*,

1752.

[14] J. Kong, S. Song, M. Yoo, G. Y. Lee, O. Kwon, J. K. Park, H. Back, G. Kim, S. H. Lee, H. Suh, K. Lee, *Nat. Commun.* **2014**, *5*, 5688.

[15] T. Heumueller, W. R. Mateker, I. T. Sachs-Quintana, K. Vandewal, J. a. Bartelt, T. M. Burke, T. Ameri, C. J. Brabec, M. D. McGehee, *Energy Environ. Sci.* **2014**, *7*, 2974.

[16] A. Tournebize, A. Rivaton, J. L. Gardette, C. Lombard, B. Pépin-Donat, S. Beaupré, M. Leclerc, *Adv. Energy Mater.* **2014**, *4*, 1.

[17] A. J. Pearson, P. E. Hopkinson, E. Couderc, K. Domanski, M. Abdi-Jalebi, N. C. Greenham, *Org. Electron. physics, Mater. Appl.* **2016**, *30*, 225.

[18] L. A. Frolova, N. P. Piven, D. K. Susarova, A. V Akkuratov, S. D. Babenko, P. A. Troshin, *Chem. Commun. (Camb).* **2015**, *51*, 2242.

[19] T. Heumueller, W. R. Mateker, A. Distler, U. F. Fritze, R. Cheacharoen, W. H. Nguyen, M. Biele, M. Salvador, M. von Delius, H.-J. Egelhaaf, M. D. McGehee, C. J. Brabec, *Energy Environ. Sci.* **2015**, *9*, 247.

[20] A. Distler, T. Sauermann, H.-J. Egelhaaf, S. Rodman, D. Waller, K.-S. Cheon, M. Lee, D. M. Guldi, *Adv. Energy Mater.* **2014**, *4*, 1300693.

[21] S. Holliday, R. S. Ashraf, A. Wadsworth, D. Baran, S. A. Yousaf, C. B. Nielsen, C.-H. Tan, S. D. Dimitrov, Z. Shang, N. Gasparini, M. Alamoudi, F. Laquai, C. J. Brabec, A. Salleo, J. R. Durrant, I. McCulloch, *Nat. Commun.* **2016**, *7*, 11585.

[22] D. Baran, R. S. Ashraf, D. A. Hanifi, M. Abdelsamie, N. Gasparini, J. A. Röhr, S. Holliday, A. Wadsworth, S. Lockett, M. Neophytou, C. J. M. Emmott, J. Nelson, C. J. Brabec, A. Amassian, T. Kirchartz, J. R. Durrant, I. Mcculloch, D. Baran, R. A. Ashraf, S. Holliday, A. Wadsworth, S. Lockett, P. J. R. Durrant, *Nat. Mater.* **2016**, *84*, 1.

[23] S. Holliday, R. S. Ashraf, A. Wadsworth, D. Baran, S. A. Yousaf, C. B. Nielsen, C.-H. Tan, S. D. Dimitrov, Z. Shang, N. Gasparini, M. Alamoudi, F. Laquai, C. J. Brabec, A. Salleo, J. R. Durrant, I. McCulloch, *Nat. Commun.* **2016**, *7*, 11585.

[24] M. T. Dang, L. Hirsch, G. Wantz, *Adv. Mater.* **2011**, *23*, 3597.

[25] H. Hintz, H.-J. Egelhaaf, L. Lüer, J. Hauch, H. Peisert, T. Chassé, *Chem. Mater.* **2011**, *23*, 145.

[26] M. Jørgensen, K. Norrman, S. A. Gevorgyan, T. Tromholt, B. Andreasen, F. C. Krebs, *Adv. Mater.* **2012**, *24*, 580.

[27] Z. Ding, J. Kettle, M. Horie, S. W. Chang, G. C. Smith, A. I. Shames, E. A. Katz, *J. Mater. Chem. A* **2016**, *4*, 7274.

[28] T. Heumueller, W. R. Mateker, I. T. Sachs-Quintana, K. Vandewal, J. a. Bartelt, T. M. Burke, T. Ameri, C. J. Brabec, M. D. McGehee, *Energy Environ. Sci.* **2014**, *7*, 2974.

[29] E. Voroshazi, B. Verreet, T. Aernouts, P. Heremans, *Sol. Energy Mater. Sol. Cells* **2011**, *95*, 1303.

[30] M. O. Reese, A. J. Morfa, M. S. White, N. Kopidakis, S. E. Shaheen, G. Rumbles, D. S. Ginley, **2008**, *92*, 746.

[31] M. Manceau, A. Rivaton, J.-L. Gardette, S. Guillerez, N. Lemaître, *Sol. Energy Mater. Sol. Cells* **2011**, *95*, 1315.

[32] Q. Burlingame, X. Tong, J. Hankett, M. Slootsky, Z. Chen, S. R. Forrest, *Energy Environ. Sci.* **2015**, *8*, 1005.

[33] T. Heumueller, T. M. Burke, W. R. Mateker, I. T. Sachs-Quintana, K. Vandewal, C. J. Brabec, M. D. McGehee, *Adv. Energy Mater.* **2015**, *5*, 1500111.

[34] T. Heumueller, W. R. Mateker, A. Distler, U. F. Fritze, R. Cheacharoen, W. H. Nguyen, M. Biele, M. Salvador, M. von Delius, H.-J. Egelhaaf, M. D. McGehee, C. J. Brabec, *Energy Environ. Sci.* **2015**, *9*, 247.

[35] L. J. a. Koster, V. D. Mihailetchi, P. W. M. Blom, *Appl. Phys. Lett.* **2006**, *88*, 52104.

[36] P. Schilinsky, C. Waldauf, C. J. Brabec, *Appl. Phys. Lett.* **2002**, *81*, 3885.

[37] L. J. A. Koster, V. D. Mihailetchi, R. Ramaker, P. W. M. Blom, *Appl. Phys. Lett.* **2005**, *86*, 1.

[38] M. M. Mandoc, F. B. Kooistra, J. C. Hummelen, B. De Boer, P. W. M. Blom, *Appl. Phys. Lett.* **2007**, *91*, 2005.

[39] W. L. Leong, S. R. Cowan, A. J. Heeger, *Adv. Energy Mater.* **2011**, *1*, 517.

[40] V. D. Mihailetchi, H. X. Xie, B. de Boer, L. J. a. Koster, P. W. M. Blom, *Adv. Funct. Mater.* **2006**, *16*, 699.

[41] M. Stephen, K. Genevičius, G. Juška, K. Arlauskas, R. C. Hiorns, *Polym. Int.* **2017**, *66*, 13.

[42] T. Heumueller, T. M. Burke, W. R. Mateker, I. T. Sachs-Quintana, K. Vandewal, C. J. Brabec, M. D. McGehee, *Adv. Energy Mater.* **2015**, *5*, 1500111.

[43] C. G. Shuttle, B. O'Regan, a. M. Ballantyne, J. Nelson, D. D. C. Bradley, J. De Mello, J. R. Durrant, *Appl. Phys. Lett.* **2008**, *92*, 90.

[44] N. Gasparini, X. Jiao, T. Heumueller, D. Baran, G. J. Matt, S. Fladischer, E. Spiecker, H. Ade, C. J. Brabec, T. Ameri, *Nat. Energy* **2016**, *1*, 16118.

[45] I. Zonno, B. Krogmeier, V. Katte, D. Lübke, A. Martinez-Otero, T. Kirchartz, *Appl. Phys. Lett.* **2016**, *109*, 183301.

[46] A. Seemann, T. Sauermann, C. Lungenschmied, O. Armbruster, S. Bauer, H. J. Egelhaaf, J. Hauch, *Sol. Energy* **2011**, *85*, 1238.

[47] S. Sweetnam, K. R. Graham, G. O. Ngongang Ndjawa, T. Heumüller, J. a. Bartelt, T. M. Burke, W. Li, W. You, A. Amassian, M. D. McGehee, *J. Am. Chem. Soc.* **2014**, *136*, 14078.

[48] J. H. Bannock, W. Xu, T. Baïssas, M. Heeney, J. C. de Mello, *Eur. Polym. J.* **2016**, *80*, 240.

[49] J. H. Bannock, N. D. Treat, M. Chabinyc, N. Stingelin, M. Heeney, J. C. de Mello, *Sci. Rep.* **2016**, *6*, 23651.

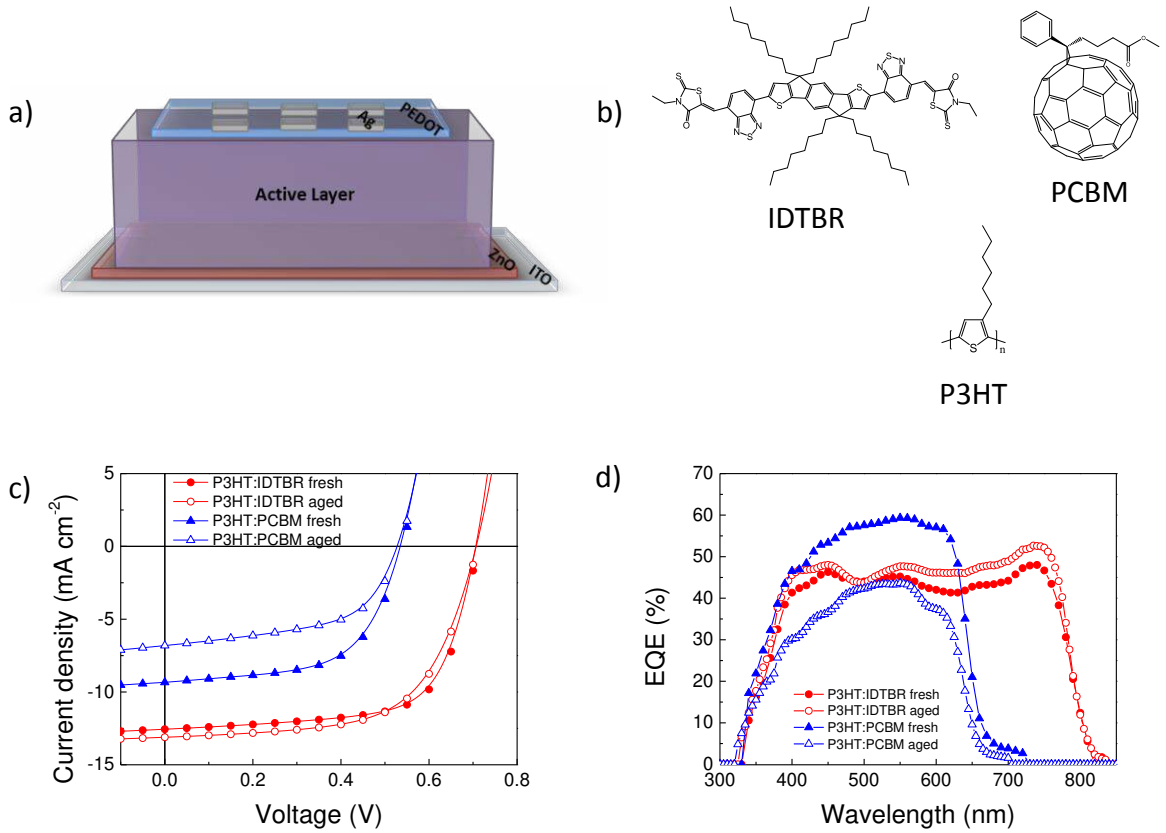

Figure 1. a) Device layout of organic solar cells fabricated in this work and b) chemical structures of the donor and acceptor molecules used as photoactive materials. c) Current-voltage (*J-V)* characteristics of P3HT:PCBM and P3HT:IDTBR solar cells under 100 mW cm^{-2} simulated solar light before and after 2000 h of light soaking. d) Spectrally resolved external quantum efficiency (EQE) of the same devices as in figure c).

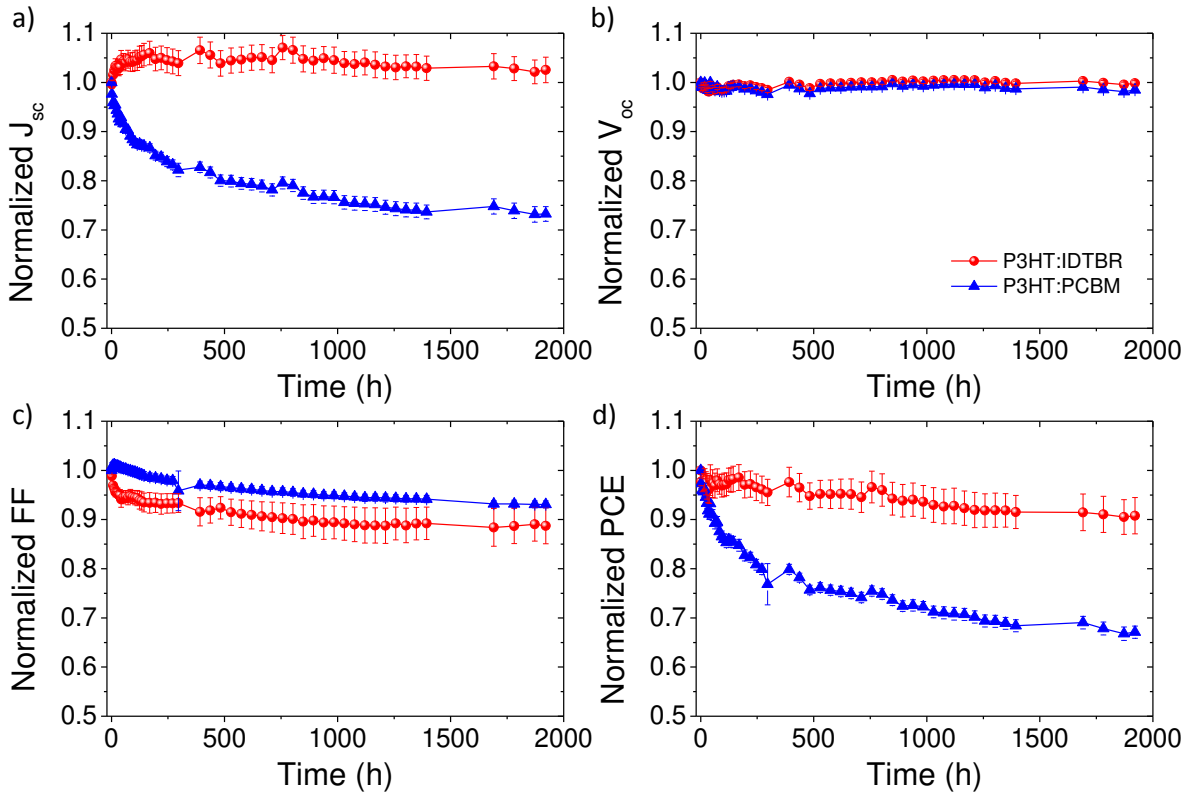

Figure 2. Normalized parameters of J_{sc}, V_{oc}, FF and *PCE* of P3HT:IDTBR and P3HT:PCBM solar cells in the course of 2000 h of light exposure. The traces for P3HT:IDTBR correspond to average values of 22 individual devices of different P3HT batches. The P3HT:PCBM data is an average of 6 devices.

Table 1. Overview of the photovoltaic and transport parameters of fresh and aged devices.

	V_{oc} [V]	J_{sc} [mA cm^{-2}]	*FF* [%]	*PCE* [%]	J_{sat} [mA cm^{-2}]	G_{MAX} [cm^{-3}s^{-1}]	G_{MPP} [%]	μ [cm^{2}V^{-1}s^{-1}]
P3HT:PCBM fresh	0.54	9.34	60	3.03	10.35	3.05×10^{21}	79	3.08×10^{-4}
P3HT:PCBM aged	0.51	6.81	58	2.02	7.86	2.43×10^{21}	75	1.65×10^{-4}
P3HT:IDTBR fresh	0.72	12.55	67	6.05	13.22	4.08×10^{21}	85	2.98×10^{-4}
P3HT:IDTBR aged	0.72	13.11	62	5.85	14.11	4.43×10^{21}	76	1.66×10^{-4}

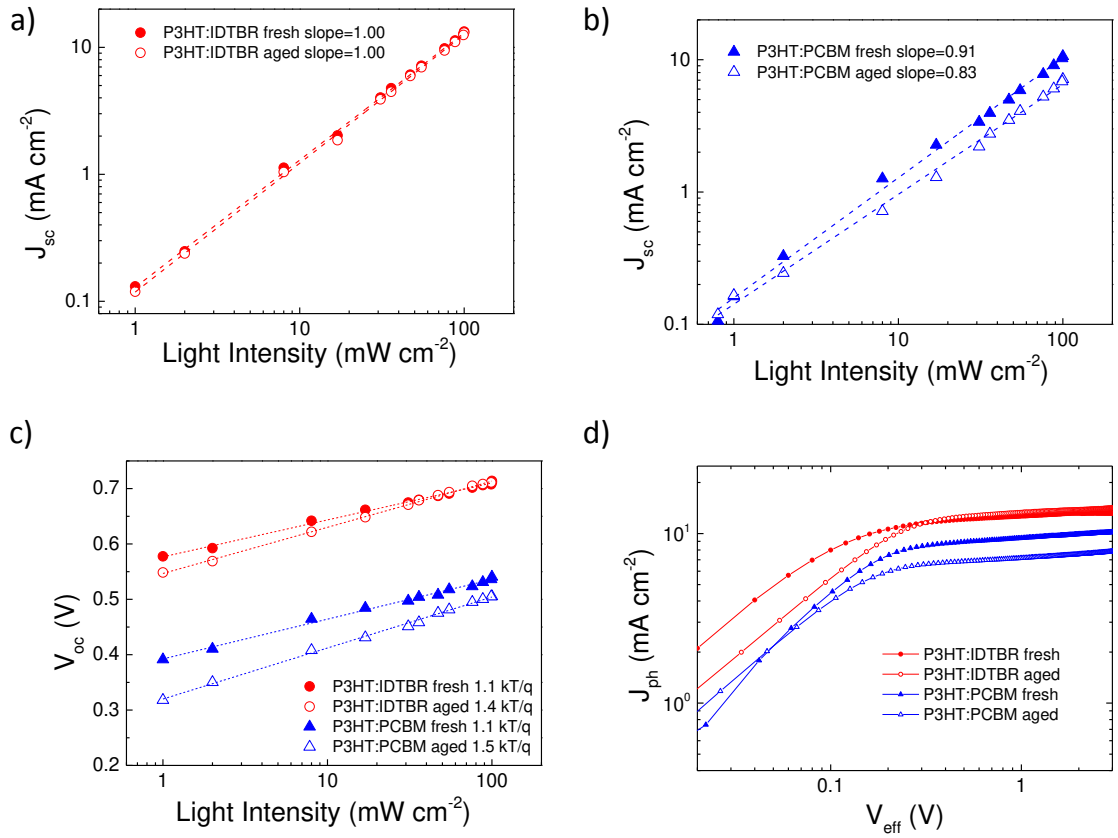

Figure 3. Short circuit current density as a function of light intensity for pristine photoaged devices of a) P3HT:IDTBR and b) P3HT:PCBM. c) Open-circuit voltage as a function of light intensity and d) photocurrent in reverse polarization for the same solar cells as in a) and b). The photocurrent J_{ph} is defined as $J_{ph} = J_l - J_d$, where J_l and J_d are the current density under illumination and in the dark, respectively, while the effective voltage V_{eff} is given by $V_{eff} = V_0 - V$, where V_0 is the compensation voltage defined as $J_{ph}(V_0)=0$, and V is the applied voltage. Photoaged devices shown here were light soaked for 2000 h.

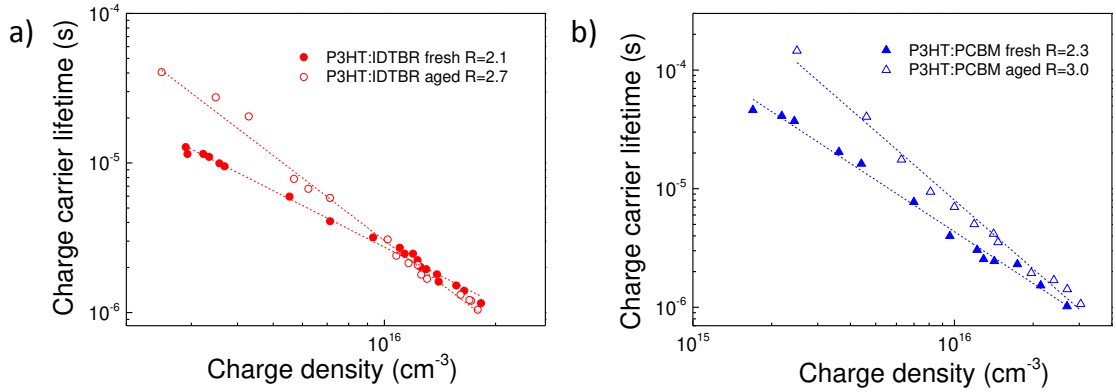

Figure 4. Charge carrier lifetime τ as a function of charge carrier density n for pristine and aged a) P3HT:IDTBR and b) P3HT:PCBM solar cells. τ was obtained from transient photovoltage (TPV) measurements, while n was calculated from charge extraction (CE) measurements under V_{oc} condition (from 0.2 to 2 suns, see ESI for details). Photoaged devices shown here were light soaked for 2000 h.

The table of contents entry should be 50−60 words long, and the first phrase should be bold. The entry should be written in the present tense and impersonal style.

We present organic solar cells based on a non-fullerene acceptor that are free of *burn-in*, the commonly observed rapid performance loss under light. The combination of enhanced efficiency and stability increases the lifetime energy yield by more than a factor of ten when compared with the same type of devices using a fullerene-based acceptor instead.

Keyword

Organic solar cells; non-fullerene acceptor; light-soaking stability; degradation; P3HT

Nicola Gasparini[1*], Michael Salvador[1,2], Sebastian Strohm[1,3], Thomas Heumueller[1], Ievgen Levchuk[1], Andrew Wadsworth[4], James H. Bannock[4], John C. de Mello[4], Hans-Joachim Egelhaaf[3], Derya Baran[5], Iain McCulloch[4,5] and Christoph J. Brabec[1,3*]

Title

Burn-in free non-fullerene based organic solar cells

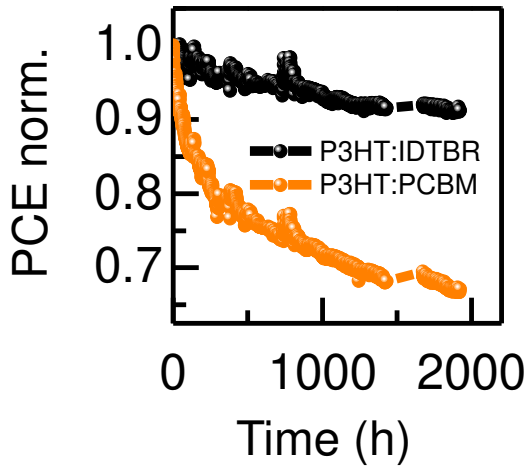

ToC figure ((Please choose one size: 55 mm broad × 50 mm high **or** 110 mm broad × 20 mm high. Please do not use any other dimensions))

Supporting information

Burn-in free non-fullerene based organic solar cells

Nicola Gasparini[1*], Michael Salvador[1,2], Sebastian Strohm[1,3], Thomas Heumueller[1], Ievgen Levchuk[1], Andrew Wadsworth[4], James H. Bannock[4], John C. de Mello[4], Hans-Joachim Egelhaaf[3], Derya Baran[5], Iain McCulloch[4,5] and Christoph J. Brabec[1,3*]

[1]Institute of Materials for Electronics and Energy Technology (I-MEET), Friedrich-Alexander-University Erlangen-Nuremberg, Martensstraße 7, 91058 Erlangen, Germany

[2]Instituto de Telecomunicações, Instituto Superior Técnico, Av. Rovisco Pais, P-1049-001 Lisboa, Portugal

[3]Bavarian Center for Applied Energy Research (ZAE Bayern), Haberstrasse 2a, 91058 Erlangen, Germany

[4]Department of Chemistry and Centre for Plastic Electronics, Imperial College London, London,SW7 2AZ, UK

[5]King Abdullah University of Science and Technology (KAUST), KAUST Solar Center (KSC), Thuwal 23955-6900, Saudi Arabia

N.G. and M.S. contributed equally to this work

Organic solar cells; non-fullerene acceptor; light-soaking stability; degradation; P3HT

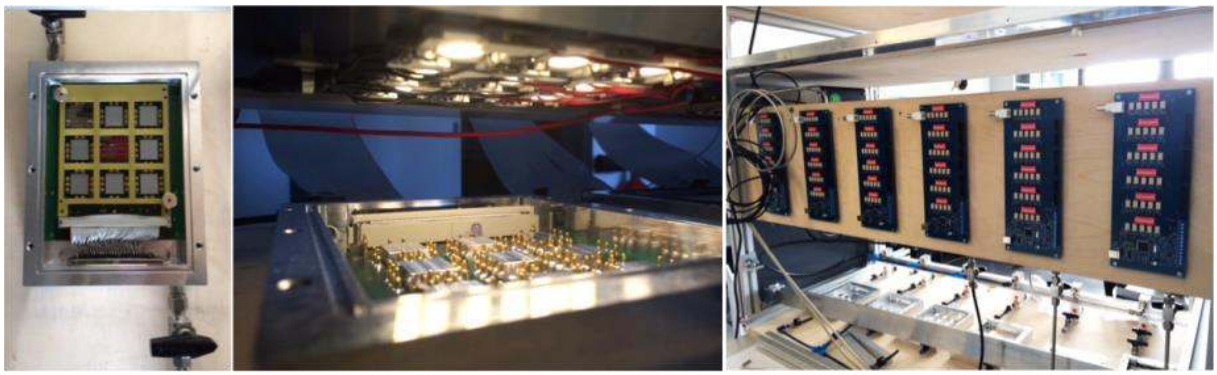

Figure S1. In-house built degradation setup used in this study. (Left) Photograph of a degradation chamber with gas in and outlets and electrical contacts for tracking the I-V performance of 54 solar cells (9 substrates, 6 solar cells per substrate). The chamber was kept under nitrogen with a continuous flow of 1 LPM. (Center) Photograph of a degradation chamber positioned under the LEDs used for light soaking experiments (the LEDs were dimmed for a better perception; the top glass cover was removed). For light-induced aging experiments, the intensity of the LEDs was adjusted to give the same short circuit current as under an AM1.5G solar simulator. (Right) Photograph providing a global overview of the whole setup, consisting of gas lines and electrical connections (6 multiplexers are attached to a wooden board) for running 6 degradation chambers at the same time.

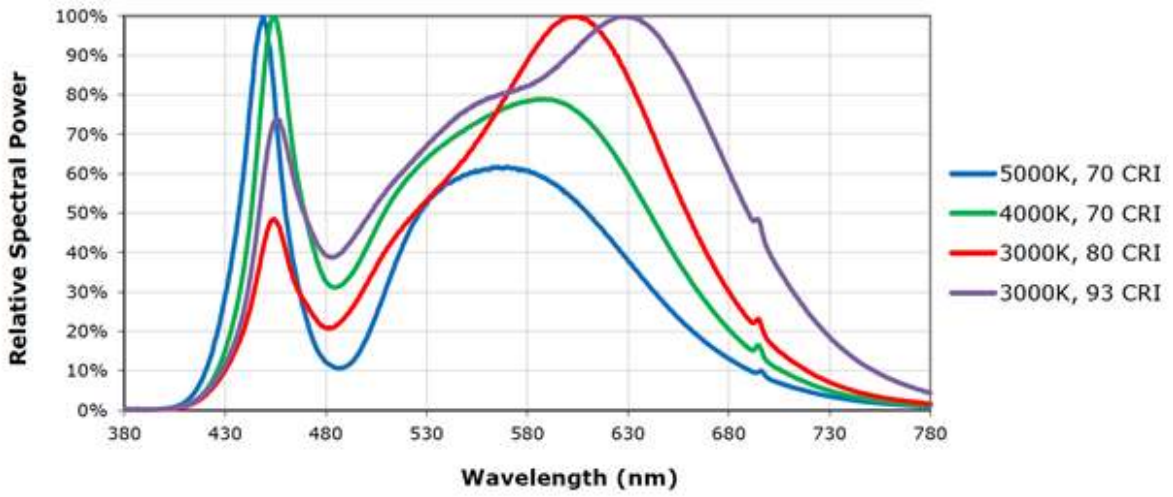

Figure S2 Light spectrum of the LEDs used in this work (3000K, 80 CRI) as extracted from the company's datasheet.

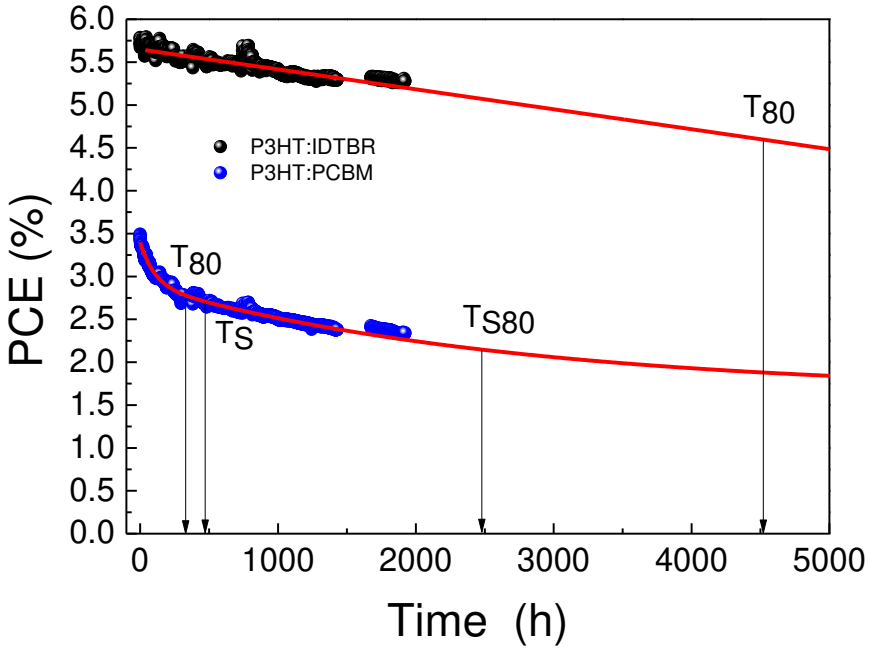

Figure S3. Power conversion efficiency as a function of light exposure time for representative P3HT:PCBM and P3HT:IDTBR solar cells. The red lines represent a linear fit and a double exponential fit to the lifetime data of IDTBR and PCBM based solar cells, respectively. The arrows highlight T_{80} (time at which the performance drops to 80% of the time zero value), T_S (burn-in time according to $T_S = -\tau_1 \ln 0.01$, where τ_1 represents the time constant of the initial exponential decay) and T_{S80} (time at which the performance drops to 80% of the T_S value). [1] The lifetime energy yield mentioned in the main text was calculated according to $LEY = \int_{t=0}^{X} \eta(t)dt \cdot 1\mathrm{kWm}^2$. The upper limit of the integral (X) was chosen to be either T_{80} or T_{S80} in the case of P3HT:PCBM. [1]

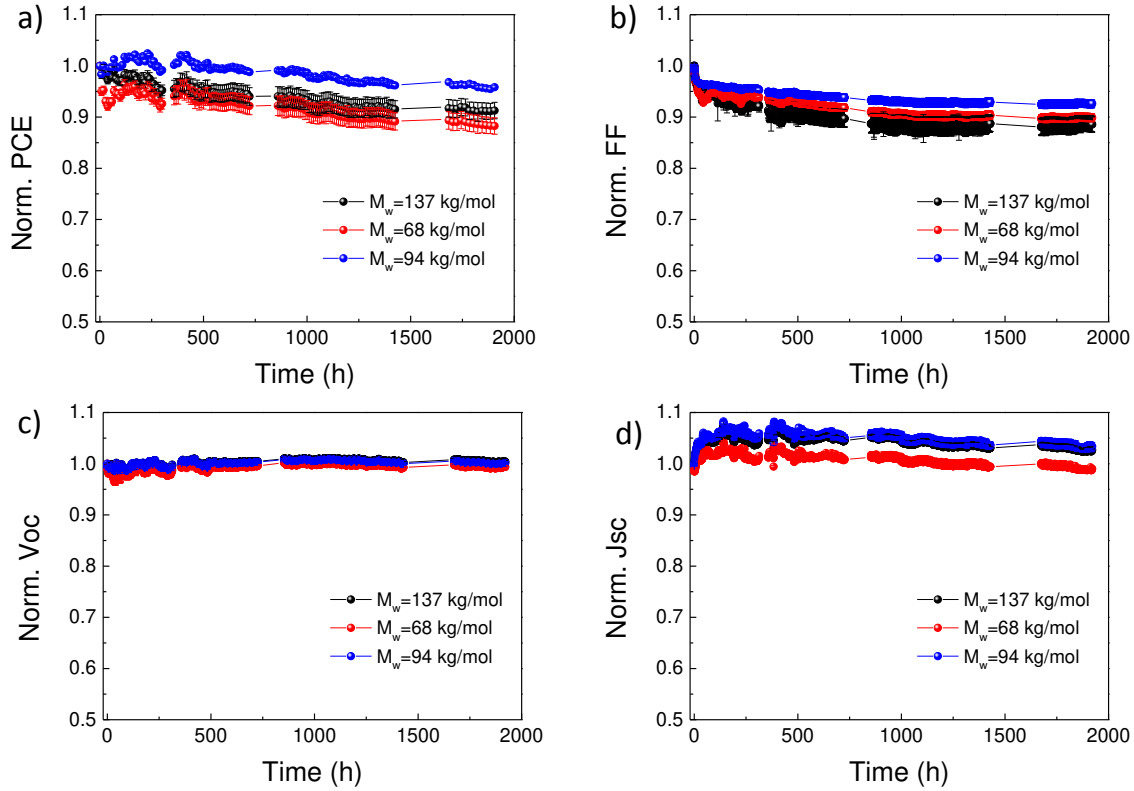

Figure S4. Temporal evolution of *PCE*, FF, V_{oc} and J_{sc} of P3HT:IDTBR solar cells during white light exposure (100 mWcm^{-2}) featuring P3HT polymers with different molecular weight. For all three cases the error bars represent the standard deviation of 6 devices. P3HT was synthesized according to previous reports. [2,3]

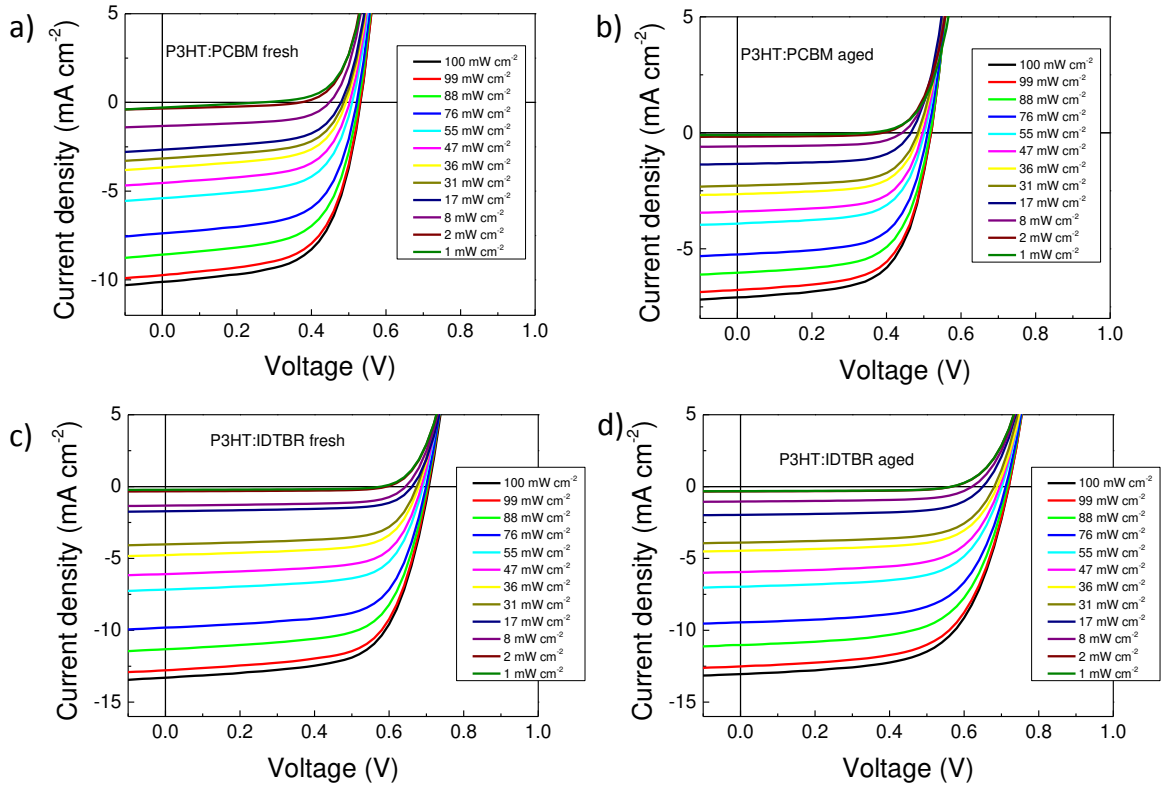

Figure S5. J-V characteristics under different light intensity for fresh (a and c) and aged (b and d, 2000 h) P3HT:PCBM and P3HT:IDTBR solar cells, respectively.

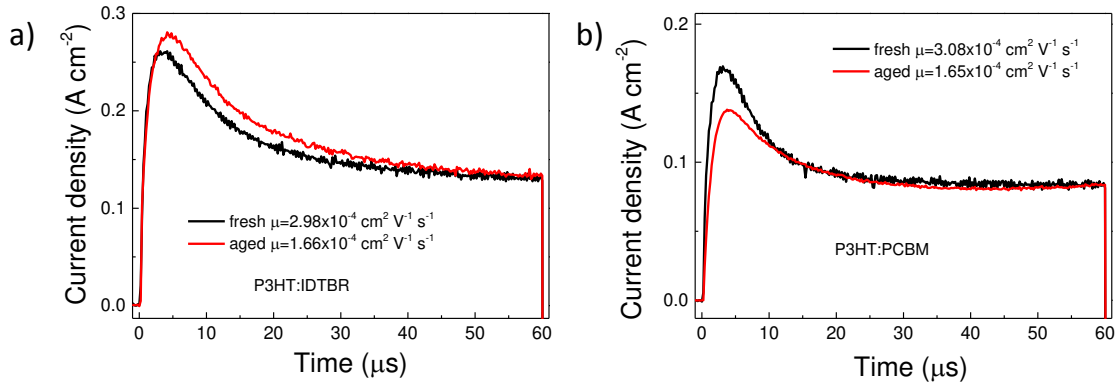

Figure S6. Photo-CELIV traces for fresh and aged (2000 h) P3HT:IDTBR (a) and P3HT:PCBM (b) solar cells, respectively.

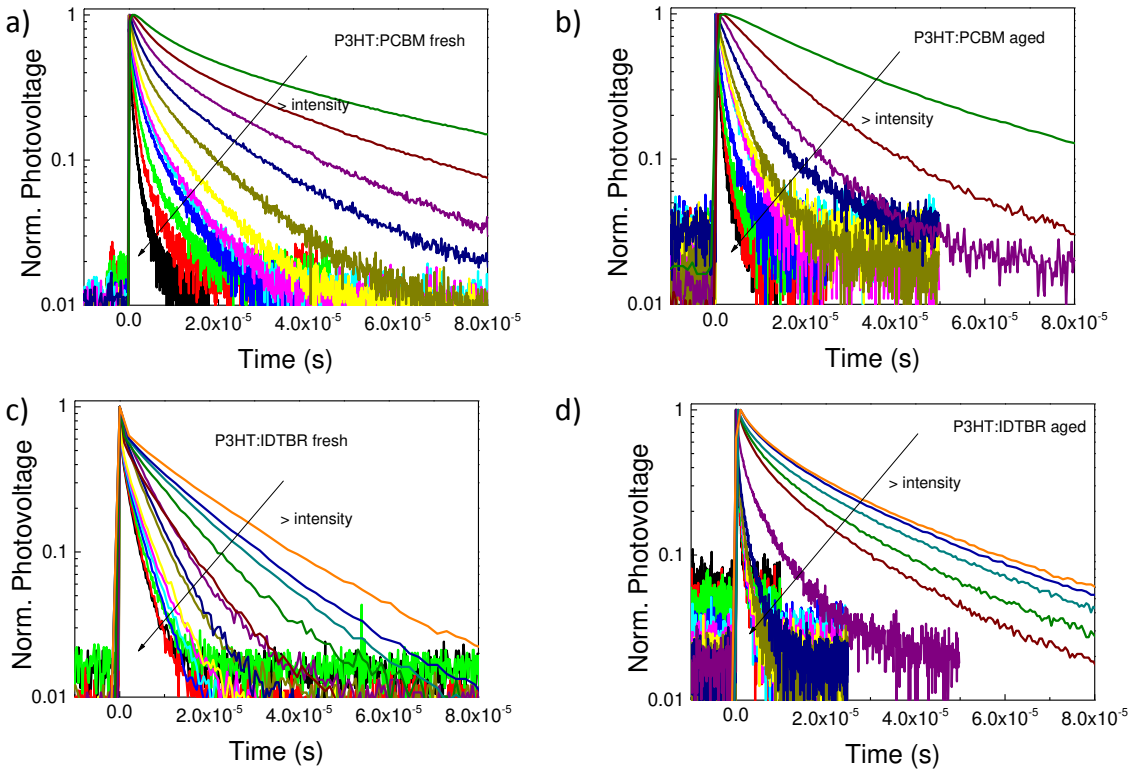

Figure S7. TPV traces under different light intensity for fresh (a and c) and aged (b and d, 2000 h) P3HT:PCBM and P3HT:IDTBR solar cells, respectively.

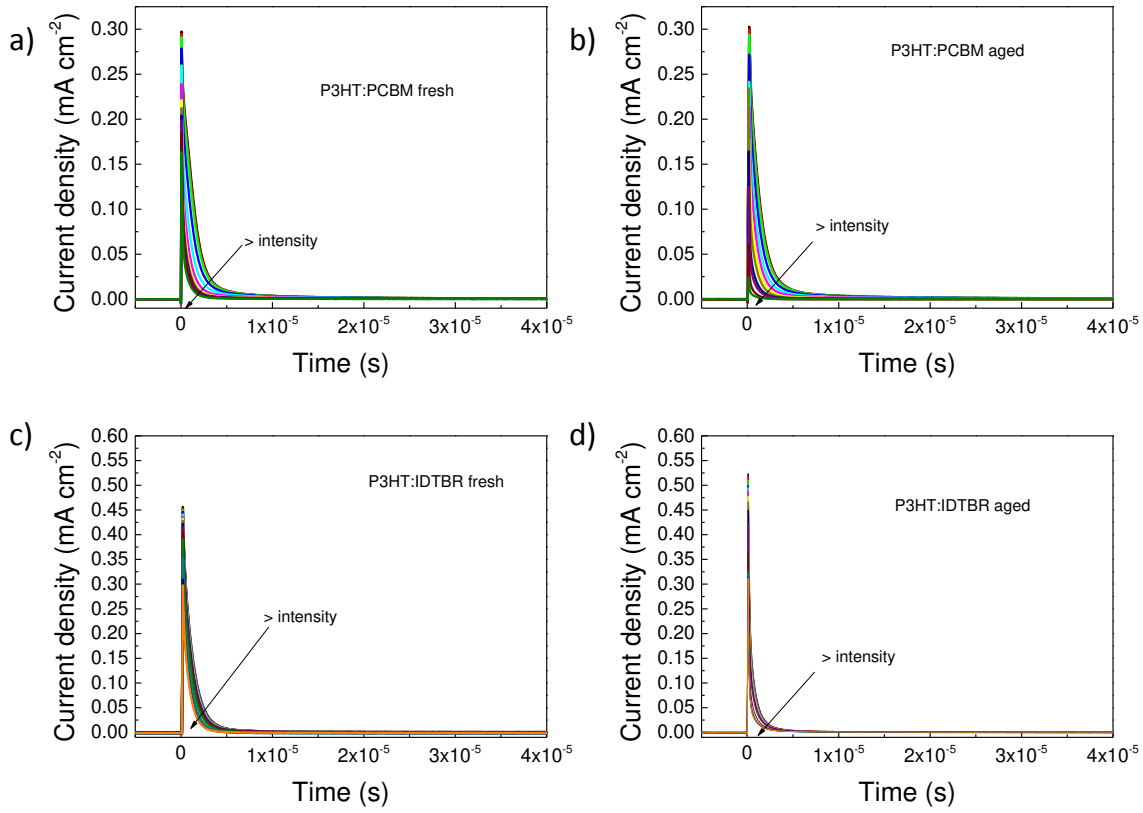

Figure S8. CE traces under different light intensity for fresh (a and c) and aged (b and d, 2000 h) P3HT:PCBM and P3HT:IDTBR solar cells, respectively.

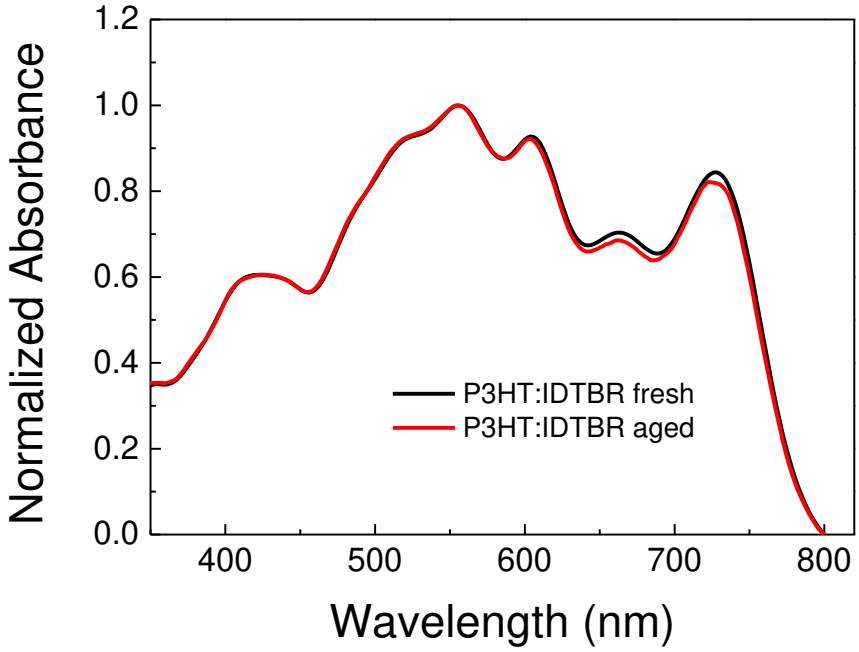

Figure S9. Normalized UV-VIS absorption profile of P3HT:IDTBR films on glass before and after light exposure (2000 h).

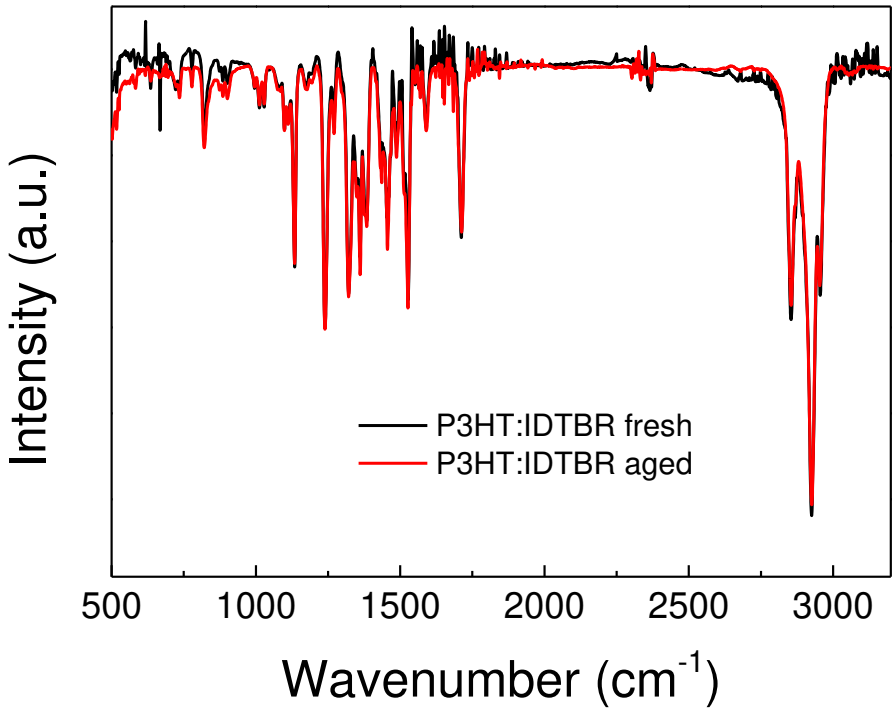

Figure S10. FTIR spectra of P3HT:IDTBR before and after light exposure (2000 h).

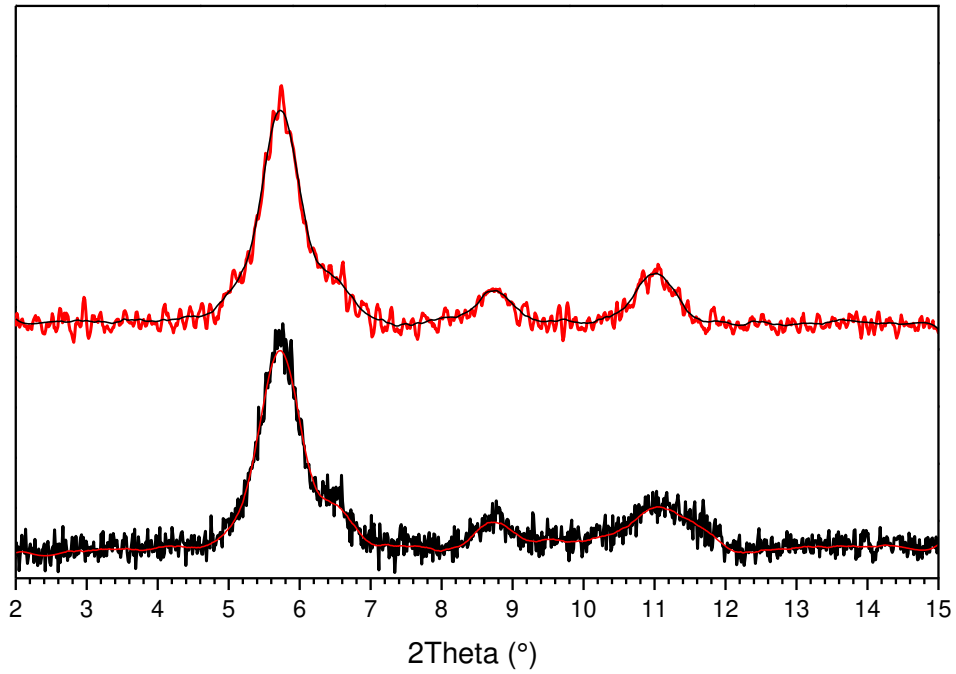

Figure S11 XRD profile of P3HT:IDTBR before and after light exposure

References

[1] R. Roesch, T. Faber, E. Von Hauff, T. M. Brown, M. Lira-Cantu, H. Hoppe, *Adv. Energy Mater.* **2015**, *5*, 1.

[2] J. H. Bannock, W. Xu, T. Bassas, M. Heeney, J. C. de Mello, *Eur. Polym. J.* **2016**, *80*, 240.

[3] J. H. Bannock, N. D. Treat, M. Chabinyc, N. Stingelin, M. Heeney, J. C. de Mello, *Sci. Rep.* **2016**, *6*, 23651.